

Coupled dynamic model of state estimation for hypersonic glide vehicle

ZHANG Kai¹, XIONG Jiajun^{2,*}, and FU Tingting²

1. Department of Graduation, Air Force Early Warning Academy, Wuhan 430019, China;

2. Early Warning Intelligence Department, Air Force Early Warning Academy, Wuhan 430019, China

Abstract: Aiming at handling complicated maneuvers or other unpredicted emergencies for hypersonic glide vehicle tracking, three coupled dynamic models of state estimation based on the priori information between guidance variables and aerodynamics are presented. Firstly, the aerodynamic acceleration acting on the target is analyzed to reveal the essence of the target's motion. Then three coupled structures for modeling aerodynamic parameters are developed by different ideas: the spiral model with a harmonic oscillator, the bank model with trigonometric functions of the bank angle and the guide model with the changing rule of guidance variables. Meanwhile, the comparison discussion is concluded to show the novelty and advantage of these models. Finally, a performance assessment in different simulation cases is presented and detailed analysis is revealed. The results show that the proposed models perform excellent properties. Moreover, the guide model produces the best tracking performance and the bank model shows the second; however, the spiral model does not outperform the maneuvering reentry vehicle (MaRV) model markedly.

Keywords: hypersonic glide vehicle, state estimation, dynamic model, aerodynamic parameter, guidance variable.

DOI: 10.21629/JSEE.2018.06.15

1. Introduction

State estimation of hypersonic glide vehicle (HGV) based on the radar measurements has been known to be a key problem for successful early-warning and interception [1]. As the HGV reenters the atmosphere, its violent maneuver behaviors induced by control system may greatly reduce the tracking accuracy [2]. Compared with employment of sophisticated filter algorithms or sensor models, good motion models largely determine the bound of estimation error and are often more beneficial to improving the estimation performance. It is greatly necessary to study the modeling problem for HGV to handle the complicated

maneuvers and improve the estimation accuracy.

The so-called wide-band kinematic models such as the white-noise acceleration, Wiener-process acceleration, Singer and Jerk model are usually applied to tracking maneuvering targets [3–6]. These models can cover many motion patterns, but they may not be sufficient to accurately estimate the states of HGV which has violent maneuver behaviors and special motion characteristics. As a matter of fact, if some prior information such as motion type or aerodynamics can be obtained beforehand, the flexibility of motion models is expected to be properly promoted. To match the skip or turn motions of HGV, Wang et al. [7–10] modeled the target's acceleration as a stochastic process with sine wave (SW) autocorrelation. The SW model can perform well when the target is skipping in vertical direction, but may show mismatch if the target turns right or left. Liang and Qin et al. [11–14] took advantage of the interacting multiple model (IMM) to handle the skip and turn maneuvers. The IMM is confirmed with excellent adaptability for maneuvering targets, whereas the problem of computation complexity has not yet been completely solved.

For the reentry vehicle flying in the atmosphere, modeling aerodynamics can effectively improve the state estimation accuracy [15, 16], which uses aerodynamic parameters to present the unknown maneuvers and builds the dynamic model by state augmentation [17–23] or input estimation [24–26]. For ballistic reentry vehicle (BRV) tracking, Li and Jilkov [15] listed a summary of dynamic models which obtain many scholars' approvals. The BRV models mainly focus on the identification of the drag coefficient (α_d) [15], ballistic coefficient ($\beta = 1/\alpha_d$) [17] or its function ($\gamma = \rho/\beta$) [24, 25], on the assumption of a particular model structure. Regarding maneuvering reentry vehicle (MaRV) tracking, a prevailing dynamic model is jointly estimated with the aerodynamic parameters (α_d , α_t and α_c) [15]. The classical dynamic models mentioned above

Manuscript received September 27, 2017.

*Corresponding author.

This work was supported by the National High-tech R&D Program of China (863 Program) (2015AA7326042; 2015AA8321471).

have clear physical meanings, but their tracking accuracy drops sharply when the model is mismatched or the aerodynamic force changes dramatically. Moreover, they generally model aerodynamic parameters by using independent Gauss or Markov processes. However, the uncoupled structures cannot entirely present the coupled aerodynamics of HGV.

As we know, the maneuvers of HGV are induced by variation of the guidance variables (i.e., bank angle and angle of attack). Based on this idea, Hough [27] used the changing law of guidance variables to deduce the aerodynamic acceleration model. However, some parameters in the model depend on off-line statistics of the flight data, which means the method is difficult to apply in practice. In order to identify the maneuver behavior on-line in the terminal phase, Karelahti et al. [28, 29] tried to estimate the guidance coefficient by assuming a certain type of the proportional guidance law. However, the terminal guidance identification usually has special structure and strong constraints, which is difficult to adapt to the HGV tracking problem in the midcourse phase.

According to the analysis mentioned above, it can be concluded that taking the priori information of guidance variables into consideration can make for modeling, but how to model the coupled aerodynamics is an urgent problem to be solved. For this purpose, three coupled dynamic models for state estimation are presented by deducing the relationship between the aerodynamics and the guidance variables. Firstly, the effect of each component of aerodynamic acceleration acting on the target is analyzed to reveal the necessity of modeling aerodynamics. Then three coupled structures of aerodynamics are designed by different particular ideas. Meanwhile, discussion of model comparison is concluded to show the novelty of the models. The performance simulation compared with the classical model in different simulation cases is presented, and detailed performance analysis is revealed later.

2. Aerodynamics analysis

2.1 Aerodynamic acceleration analysis

The target's vector motion can be described by the following equation:

$$\ddot{\mathbf{r}} = \mathbf{a}_A + \mathbf{a}_G \quad (1)$$

where \mathbf{a}_A is the aerodynamic acceleration; \mathbf{a}_G is the gravity acceleration. The \mathbf{a}_G can be estimated via target's location indirectly, but \mathbf{a}_A which directly determines the maneuvers is unknown. The key to the state estimation problem of HGV is how to model \mathbf{a}_A . For facilitation of analysis, \mathbf{a}_A is generally decomposed in the velocity-turn-climb (VTC) coordinate system (CS) [15]:

$$\mathbf{a}_A^{(\text{VTC})} = -D\mathbf{u}_v + L(-\mathbf{u}_t \sin \varphi + \mathbf{u}_c \cos \varphi) \quad (2)$$

with

$$\begin{cases} D = \frac{1}{2}\rho v^2 \cdot \frac{C_D(\alpha)S}{m} \\ L = \frac{1}{2}\rho v^2 \cdot \frac{C_L(\alpha)S}{m} \end{cases} \quad (3)$$

where \mathbf{u}_v , \mathbf{u}_t and \mathbf{u}_c are triplet of unit vectors which define the orthogonal body frame of VTC-CS; φ and α are the bank angle and angle of attack, respectively; D and L are the drag acceleration and lift acceleration, respectively; S and m are the target's reference area and mass, respectively; v is the speed; ρ is the atmospheric density; $C_D(\alpha)$ and $C_L(\alpha)$ are the drag coefficient and lift coefficient, respectively, which are functions of α [30].

In order to reveal the relationship between \mathbf{a}_A and the guidance variables, the time derivatives of \mathbf{a}_A can be expressed as

$$\dot{\mathbf{a}}_A = \underbrace{\boldsymbol{\omega} \times \mathbf{a}_A}_a + \underbrace{\dot{\varphi} \mathbf{u}_v \times \mathbf{a}_A}_b - \underbrace{\dot{D} \mathbf{u}_v}_c + \underbrace{\dot{L}(-\mathbf{u}_t \sin \varphi + \mathbf{u}_c \cos \varphi)}_d \quad (4)$$

where $\boldsymbol{\omega}$ indicates the turn rate of the target. Defining \mathbf{F} as the maneuver plane, it is clear that $\boldsymbol{\omega}$ is orthogonal to \mathbf{F} . The sketch of the derivative vector is shown in Fig. 1, and deeper information of each term in (4) is given below:

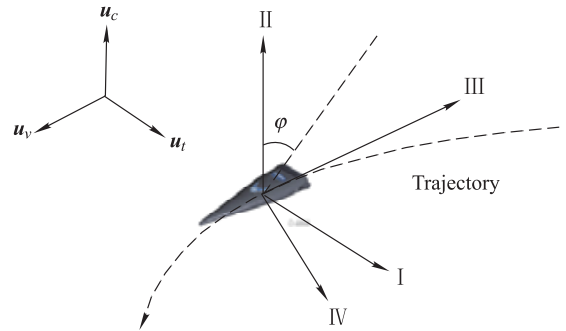


Fig. 1 Sketch of derivative vector

I denotes the motion in the plane \mathbf{F} . This term is perpendicular to $\boldsymbol{\omega}$ and \mathbf{a}_A . With the hypothesis of constant lift and drag (i.e., no banking), the motion is confined to the so-called coordinated turn model;

II denotes the motion out of the plane \mathbf{F} , which is attributed to the rotation of the lift vector. With the hypothesis of constant $\dot{\varphi}$, the motion is confined to the so-called spiral model;

III is attributed to variation of the drag. This term contributes to the motion inside the plane \mathbf{F} ;

IV is attributed to variation of the lift. This term contributes to out-of-plane motion.

The analysis shows that the complicated maneuvers of HGV are composed of some simple motion models. Besides, guidance variables conduct these terms via lift and drag indirectly. It means that consideration of relationship between \mathbf{a}_A and guidance variables can contribute to handling complicated maneuvers of HGV.

2.2 Aerodynamic parameter definition

Unlike accounting for the drag in the BRV model, both the drag and lift should be considerate in the HGV model. A popular approach to describe \mathbf{a}_A is to use a kinematic state-dependent factor $\rho v^2/2$ to transform these uncertainties (C_D , C_L , S , and m , etc) into the format of so-called aerodynamic parameters, and \mathbf{a}_A can be described in the east-north-up (ENU) -CS as follows [15]:

$$\mathbf{a}_A^{(\text{ENU})} = \begin{bmatrix} A_x \\ A_y \\ A_z \end{bmatrix} = \frac{1}{2} \rho v^2 \begin{bmatrix} \frac{v_x}{v} & -\frac{v_y}{v_g} & -\frac{v_x v_z}{v v_g} \\ \frac{v_y}{v} & \frac{v_x}{v_g} & -\frac{v_y v_z}{v v_g} \\ \frac{v_z}{v} & 0 & \frac{v_g}{v} \end{bmatrix} \begin{bmatrix} -\alpha_v \\ \alpha_t \\ \alpha_c \end{bmatrix} \quad (5)$$

where $v = \sqrt{v_x^2 + v_y^2 + v_z^2}$, $v_g = \sqrt{v_x^2 + v_y^2}$. v_x , v_y and v_z are the components of v in the ENU-CS, respectively; A_x , A_y and A_z are the components of \mathbf{a}_A in the ENU-CS, respectively; α_v , α_t and α_c are the drag parameter, turn force parameter and climb force parameter along the corresponding direction of three axes in the VTC-CS, respectively.

Aerodynamic parameters can present the target's maneuvers in each direction directly: (i) $\alpha_t > 0$ (or $\alpha_t < 0$) represents turning left (or right); (ii) $\alpha_c > 0$ (or $\alpha_c < 0$) represents climbing (or diving). Referring to (2), (3) and (5), the relationship between aerodynamic parameters and guidance variables can be expressed as follows:

$$\begin{bmatrix} \alpha_v \\ \alpha_t \\ \alpha_c \end{bmatrix} = \frac{S}{m} \cdot \begin{bmatrix} C_D(\alpha) \\ -C_L(\alpha) \sin \varphi \\ C_L(\alpha) \cos \varphi \end{bmatrix}. \quad (6)$$

It can be found that the variation of aerodynamic parameters is determined by guidance variables α and φ . Meanwhile, the guidance variables lead to the coupling between aerodynamic parameters. The classical MaRV model (MM) in [17–26] is a decoupled way in essence. Hence, in the next section we try different ways to take the coupled relationship into account for aerodynamic modeling.

3. Aerodynamic modeling

In this section, three original dynamic models with different coupled structures, which have potential to express the

aerodynamics of HGV, are described in the following sub-sections.

3.1 Spiral model

The key idea of spiral model (SM) is to assume the HGV undergoing the spiral motion based on the moment equilibrium [20, 21]. The SM accounts for the correlation between α_t and α_c to improve estimation accuracy. According to (6) and assuming α is nearly constant, the derivatives of α_t and α_c can be expressed as follows:

$$\begin{bmatrix} \dot{\alpha}_t \\ \dot{\alpha}_c \end{bmatrix} = \begin{bmatrix} -\frac{C_L(\alpha)S}{m} \cos \varphi \cdot \dot{\varphi} \\ -\frac{C_L(\alpha)S}{m} \sin \varphi \cdot \dot{\varphi} \end{bmatrix}. \quad (7)$$

According to (7), a steady harmonic oscillator existing between α_t and α_c can be concluded as follows:

$$\begin{bmatrix} \dot{\alpha}_t \\ \dot{\alpha}_c \end{bmatrix} = \begin{bmatrix} 0 & -\varpi \\ \varpi & 0 \end{bmatrix} \begin{bmatrix} \alpha_t \\ \alpha_c \end{bmatrix} \quad (8)$$

where $\varpi = \dot{\varphi}$ is the spiral rate.

In (8), the harmonic oscillator uses the spiral rate ϖ to reflect the severity of maneuvers. ϖ can be used as the augmented state variable to represent the coupled relationship between α_t and α_c . As a consequence, modeling the statistical property of ϖ by a first-order Markov process, the dynamic of augmented parameters in the SM can be expressed as

$$\begin{bmatrix} \dot{\alpha}_v \\ \dot{\alpha}_t \\ \dot{\alpha}_c \\ \dot{\varpi} \end{bmatrix} = \begin{bmatrix} -\lambda_v & 0 & 0 & 0 \\ 0 & 0 & -\varpi & 0 \\ 0 & \varpi & 0 & 0 \\ 0 & 0 & 0 & -\lambda_\varpi \end{bmatrix} \begin{bmatrix} \alpha_v \\ \alpha_t \\ \alpha_c \\ \varpi \end{bmatrix} + \begin{bmatrix} w_v \\ w_t \\ w_c \\ w_\varpi \end{bmatrix} \quad (9)$$

where w_v , w_t , w_c and w_ϖ are zero-mean Gaussian white noise sequences for the corresponding augmented parameters; λ_ϖ is the maneuver frequency for ϖ .

3.2 Bank model

Like the SM, the bank model (BM) also takes the correlation between α_t and α_c into consideration. The difference is that the latter uses the bank angle φ to present trigonometric functions between α_t and α_c .

The BM assumes that the HGV yaws left or right induced by the bank to turn (BTT) control. It means that the bank between lateral motion and lift motion is indicated by bank angle φ . According to this idea, the α_t and α_c are modified by (6) as follows:

$$\begin{bmatrix} \alpha_t \\ \alpha_c \end{bmatrix} = \begin{bmatrix} -\alpha_l \sin \varphi \\ \alpha_l \cos \varphi \end{bmatrix} \quad (10)$$

where $\alpha_l = C_L(\alpha)S/m$ is defined as the lift parameter.

According to (10), the modifications aligned with α_l and φ show a concise structure for α_t and α_c . We can use α_l and φ as the modified parameters to represent the negative correlation between α_t and α_c . Therefore the modified parameters in the BM are presented as follows:

$$\begin{bmatrix} \alpha_v \\ \alpha_l \\ k \end{bmatrix} = \begin{bmatrix} \frac{C_D S}{m} \\ \frac{C_L S}{m} \\ \sin \varphi \end{bmatrix} \quad (11)$$

where $k = \sin \varphi$ is used to substitute for trigonometric functions (i.e., $\sin \varphi$ or $\cos \varphi$).

Referring to (5), (6) and (11), the components of $\mathbf{a}_A^{(\text{ENU})}$ resulting from the modified parameters are represented by

$$\mathbf{a}_A^{(\text{ENU})} = \begin{bmatrix} A_x \\ A_y \\ A_z \end{bmatrix} = \frac{1}{2} \rho v^2 \mathbf{T}_{\text{VTC}}^{\text{ENU}}(\mathbf{v}) \begin{bmatrix} -\alpha_v \\ -\alpha_l k \\ \alpha_l \sqrt{1-k^2} \end{bmatrix}. \quad (12)$$

Note that $\sqrt{1-k^2}$ in the right-hand side of (12) is nonlinear and not suitable for filtering. It can be approximated as the Taylor expansion equation:

$$\sqrt{1-k^2} \approx 1 - \frac{k^2}{2} - \frac{k^4}{8}. \quad (13)$$

The statistical properties of aerodynamic parameters caused by maneuvers are represented by the first-order Markov processes. The dynamic of augmented parameters in the BM is expressed as follows:

$$\begin{bmatrix} \dot{\alpha}_v \\ \dot{\alpha}_l \\ \dot{k} \end{bmatrix} = \begin{bmatrix} -\lambda_v & 0 & 0 \\ 0 & -\lambda_l & 0 \\ 0 & 0 & -\lambda_k \end{bmatrix} \begin{bmatrix} \alpha_v \\ \alpha_l \\ k \end{bmatrix} + \begin{bmatrix} w_v \\ w_l \\ w_k \end{bmatrix} \quad (14)$$

where w_l and w_k are zero-mean Gaussian white noise sequences for the corresponding augmented parameters; λ_l and λ_k are the maneuver frequency for α_l and k , respectively.

3.3 Guide model

The guide model (GM) no longer simply treats aerodynamic parameters as the random processes, but models them by changing rule of guidance variables α and φ . For lacking information of the target's control system, we can assume that variation of α and φ obeys the first-order time-delay processes as follows [27]:

$$\begin{cases} \dot{\alpha} = \frac{1}{\tau_\alpha}(\alpha_g - \alpha) \\ \dot{\varphi} = \frac{1}{\tau_\varphi}(\varphi_g - \varphi) \end{cases} \quad (15)$$

where τ_α and τ_φ are the time constants which represent the changing speed of corresponding guidance variables; α_g and φ_g are the guidance commands which represent the expected values of corresponding guidance variables.

Since the HGV glides at high speed in near space, sharp adjustment of α_g may make aerodynamic characteristics complex and increase burden on the target's control and thermal protection system. Hence, α is usually used as an auxiliary guidance variable to perform small-scale adjustment based on the nominal angle of attack [31]. It means that $\alpha_g - \alpha$ is very small, so $C_D(\alpha_g)$ and $C_L(\alpha_g)$ can be approximated as the first-order Taylor expansion equations:

$$\begin{cases} C_D(\alpha_g) \cong C_D(\alpha) + \frac{dC_D(\alpha)}{d\alpha}(\alpha_g - \alpha) \\ C_L(\alpha_g) \cong C_L(\alpha) + \frac{dC_L(\alpha)}{d\alpha}(\alpha_g - \alpha) \end{cases} \quad (16)$$

Referring to (15) and (16), the derivatives of α_v and α_l can be expressed as

$$\begin{cases} \dot{\alpha}_v = \frac{S}{m} \frac{dC_D(\alpha)}{d\alpha} \cdot \frac{1}{\tau_\alpha}(\alpha_g - \alpha) \cong \\ \frac{1}{\tau_\alpha} \frac{S}{m} [C_D(\alpha_g) - C_D(\alpha)] = \\ \frac{1}{\tau_\alpha}(\alpha_{vg} - \alpha_v) \\ \dot{\alpha}_l = \frac{S}{m} \frac{dC_L(\alpha)}{d\alpha} \cdot \frac{1}{\tau_\alpha}(\alpha_g - \alpha) \cong \\ \frac{1}{\tau_\alpha} \frac{S}{m} [C_L(\alpha_g) - C_L(\alpha)] \cong \\ \frac{1}{\tau_\alpha}(\alpha_{lg} - \alpha_l) \end{cases} \quad (17)$$

where α_{vg} and α_{lg} are the guidance commands of α_v and α_l , respectively.

According to (4), the derivatives of α_t and α_c can be expressed as

$$\begin{cases} \dot{\alpha}_t = -\dot{\alpha}_l \sin \varphi - \alpha_l \cos \varphi \cdot \dot{\varphi} \\ \dot{\alpha}_c = \dot{\alpha}_l \cos \varphi - \alpha_l \sin \varphi \cdot \dot{\varphi} \end{cases} \quad (18)$$

Substitute (15) and (17) into (18):

$$\begin{cases} \dot{\alpha}_t = -\frac{\sin \varphi}{\tau_\alpha}(\alpha_{lg} - \alpha_l) - \frac{\alpha_l \cos \varphi}{\tau_\varphi}(\varphi_g - \varphi) = \\ \frac{\alpha_t}{\tau_\alpha} \left(\frac{\alpha_{lg}}{\alpha_l} - 1 \right) - \frac{\alpha_c}{\tau_\varphi}(\varphi_g - \varphi) \\ \dot{\alpha}_c = \frac{\cos \varphi}{\tau_\alpha}(\alpha_{lg} - \alpha_l) - \frac{\alpha_l \sin \varphi}{\tau_\varphi}(\varphi_g - \varphi) = \\ \frac{\alpha_c}{\tau_\alpha} \left(\frac{\alpha_{lg}}{\alpha_l} - 1 \right) + \frac{\alpha_t}{\tau_\varphi}(\varphi_g - \varphi) \end{cases} \quad (19)$$

In this way, the dynamic of augmented parameters in the GM can be built by (17) and (19):

$$\begin{cases} \dot{\alpha}_v = \frac{1}{\tau_\alpha}(\alpha_{vg} - \alpha_v) + w_v \\ \dot{\alpha}_t = \frac{\alpha_t}{\tau_\alpha}(\frac{\alpha_{lg}}{\alpha_l} - 1) - \frac{\alpha_c}{\tau_\varphi}(\varphi_g - \varphi) + w_t \\ \dot{\alpha}_c = \frac{\alpha_c}{\tau_\alpha}(\frac{\alpha_{lg}}{\alpha_l} - 1) + \frac{\alpha_t}{\tau_\varphi}(\varphi_g - \varphi) + w_c \end{cases} \quad (20)$$

The guidance commands α_{vg} , α_{lg} and φ_g are time-varying parameters which result in the target maneuvers. To ensure availability and self-adaptability of the GM, it is necessary to identify the guidance commands online. For this reason, the guidance commands are assumed to be constant within a short time. Combining (15) and (17), the guidance commands are approximated on account of the estimated aerodynamic parameters:

$$\begin{cases} \alpha_{vg}(k+1) \cong \tau_\alpha \hat{\alpha}_v(k) + \hat{\alpha}_v(k) \\ \alpha_{lg}(k+1) \cong \tau_\alpha \hat{\alpha}_l(k) + \hat{\alpha}_l(k) \\ \varphi_g(k+1) \cong \tau_\varphi \hat{\varphi}(k) + \hat{\varphi}(k) \end{cases} \quad (21)$$

Note that $\hat{\alpha}_v(k)$, $\hat{\alpha}_l(k)$, $\hat{\varphi}(k)$ in (21) are unknown, and the moving average method is used to eliminate these unknown parameters [26]. Assuming that the window length is n , the moving average of guidance commands can be expressed as

$$\begin{cases} \alpha_{vg}(k+n) = \int_{kT}^{(k+n-1)T} \frac{\tau_\alpha \hat{\alpha}_v + \hat{\alpha}_v}{(n-1)T} dt \cong \\ \tau_\alpha \frac{\hat{\alpha}_v(k+n-1) - \hat{\alpha}_v(k)}{(n-1)T} + \sum_{i=0}^{n-1} \frac{\hat{\alpha}_v(k+i)}{n} \\ \alpha_{lg}(k+n) = \int_{kT}^{(k+n-1)T} \frac{\tau_\alpha \hat{\alpha}_l + \hat{\alpha}_l}{(n-1)T} dt \cong \\ \tau_\alpha \frac{\hat{\alpha}_l(k+n-1) - \hat{\alpha}_l(k)}{(n-1)T} + \sum_{i=0}^{n-1} \frac{\hat{\alpha}_l(k+i)}{n} \\ \varphi_g(k+n) = \int_{kT}^{(k+n-1)T} \frac{\tau_\varphi \hat{\varphi} + \hat{\varphi}}{(n-1)T} dt \cong \\ \tau_\varphi \frac{\hat{\varphi}(k+n-1) - \hat{\varphi}(k)}{(n-1)T} + \sum_{i=0}^{n-1} \frac{\hat{\varphi}(k+i)}{n} \end{cases} \quad (22)$$

Note that the guidance command in (22) cannot be identified in the filter startup phase ($k < n$); therefore it can be assumed that the target does not maneuver (i.e., $\alpha_g = \alpha$ & $\varphi_g = \varphi$), the GM is simplified to Gaussian-Wiener model consequently.

4. Discussion of model comparison

In summary, the dynamic models mentioned above rely on the following idea: quantify the unknown aerodynamic accelerations \mathbf{a}_A through aerodynamic parameters

or their variants scaled by a kinematic state-dependent factor $\rho v^2/2$, then model these parameters as the well-designed process and augment the state vector by them. In order to reveal the intrinsic difference from other similar models, four dynamic models (i.e., the MM [15] and the proposed models) shown in Table 1 are discussed below.

The MM gives rise to independence of the aerodynamic parameters (α_d , α_t and α_c) in three channels. Its uncoupled structure is deemed to accommodate wide-band variation, but loses some prior information as well.

Table 1 Dynamic models for the HGV

Model	State variable \mathbf{X}
MM	$[x, y, z, v_x, v_y, v_z, \alpha_v, \alpha_t, \alpha_c]^T$
SM	$[x, y, z, v_x, v_y, v_z, \alpha_v, \alpha_t, \alpha_c, \varpi]^T$
BM	$[x, y, z, v_x, v_y, v_z, \alpha_v, \alpha_l, k]^T$
GM	$[x, y, z, v_x, v_y, v_z, \alpha_v, \alpha_t, \alpha_c]^T$

Based on α_d , α_t and α_c , the SM uses the additional augmented state ϖ to cover the spiral motion between turn and climb. It assumes that ω_s varies when HGV is maneuvering. This consideration may contribute to the improvement of estimation accuracy. However, it also increases complexity because of a thirteen-state vector.

The BM focuses on the feature of bank motion with coupled kinematic equation $\alpha_l^2 = \alpha_t^2 + \alpha_c^2$ and have clear physical meanings: α_v and α_l represent the drag and lift, respectively; φ indicates the direction of lift. Through this form of parametric modeling, the BM considers the coupled relationship between α_t and α_c , but it does not increase the computational complexity.

The GM models aerodynamic parameters by the first-order time-delay process of guidance variables indirectly. Analyzing (20) under different flight conditions, the following conclusions can be drawn: i) When the HGV is not maneuvering, guidance variables keep constant (i.e., $\alpha_g = \alpha$ and $\varphi_g = \varphi$), (20) can be simplified as the Gauss-Wiener model; ii) When the HGV is climbing (or diving), α keeps constant and φ changes (i.e., $\alpha_g = \alpha$ and $\varphi_g \neq \varphi$), (20) can be simplified as a model related with α_{vg} and α_{lg} ; iii) When the HGV is turning left (or right), α changes and φ keeps constant (i.e., $\alpha_g \neq \alpha$ and $\varphi_g = \varphi$), (20) can be simplified as a model related with φ_g . In summary, it is clear that the GM can match the maneuver adaptively and may help to improve the estimation accuracy.

In a word, although these models are augmented by parameters similarly, the MM has the loosest structure. By consideration of prior information, the coupled models mentioned in this paper should have better performance than the MM.

5. Filtering framework

The state equation $\mathbf{f}(\mathbf{X})$ of \mathbf{X} is discretized for filtering by the following equation:

$$\mathbf{X}_{k|k+1} = \mathbf{X}_{k|k} + \mathbf{f}(\mathbf{X}_{k|k}, t_k)t + \frac{1}{2}\mathbf{F}(\mathbf{X}_{k|k}) \cdot \mathbf{f}(\mathbf{X}_{k|k}, t_k)t^2 \quad (23)$$

where t is the sampling period; $\mathbf{F}(\mathbf{X}_{k|k})$ is the Jacobian matrix of $\mathbf{f}(\mathbf{X}_{k|k}, t_k)$ with respect to $\mathbf{X}_{k|k}$.

The measurement vector obtained in the spherical CS is defined as $\mathbf{Z} = (R, A, E)^T$, where R is the radial distance, A is the pitch angle, and E is the azimuth. According to the relationship between the ENU-CS and the spherical CS, the measurement equation is expressed as follows:

$$\mathbf{Z} = \mathbf{h}(\mathbf{X}) + \mathbf{w} = \begin{bmatrix} \sqrt{x^2 + y^2 + z^2} \\ \arctan(x/y) \\ \arctan\left(\frac{z}{\sqrt{x^2 + y^2}}\right) \end{bmatrix} + \begin{bmatrix} n_R \\ n_A \\ n_E \end{bmatrix} \quad (24)$$

where n_R , n_A and n_E are zero mean Gaussian white noise sequences for the observations.

6. Simulation and performance comparison

This section presents the overall perspective of comparative performance assessment for the proposed dynamic models. Discussion in the following attempts to reveal their validity and utility for state estimation.

6.1 Simulation facilities and criteria

Simulation environment is designed as follows: (i) Target parameters: a typical vehicle CAV-H [32] is applied to the simulation, the predetermined glide duration is set to 180 s, strong maneuver happens at $t \approx 35$ s and weak maneuver happens at $t \approx 90$ s; (ii) Sensor parameters: the measurements are generated from the simulation trajectory with zero-mean white noise, and the standard deviation R denotes 500 m in range, 0.01 rad in pitch angle and 0.01 rad in azimuth, the sampling period $T = 0.1$ s.

Four dynamic models mentioned in Section 4 are compared. The Monte Carlo simulation is performed 100 times for the simulation example. In order to compare the performance explicitly, the root mean square errors (RMSEs) of each case are calculated. Note that α_t and α_c of the BM are calculated indirectly from the estimated states α_l and k by (11).

6.2 Performance comparison

Fig. 2 and Fig. 3 show the position and velocity RMSE results. It can be seen that: (i) When the target is maneuvering strongly, the estimation errors of the four models become somewhat large, and then gradually decrease.

The estimation errors of the proposed models are approximately 95%, 80% and 75% of that in the MM. Clearly, the convergence speed of GM is fastest; (ii) When the target is maneuvering weakly, the estimation errors of MM and SM increase significantly, but the position estimation errors of BM and GM fluctuate softly, and their velocity estimation errors are approximately 75% and 60% of that in the MM; (iii) When the target does not maneuver, the difference in performance is not obvious.

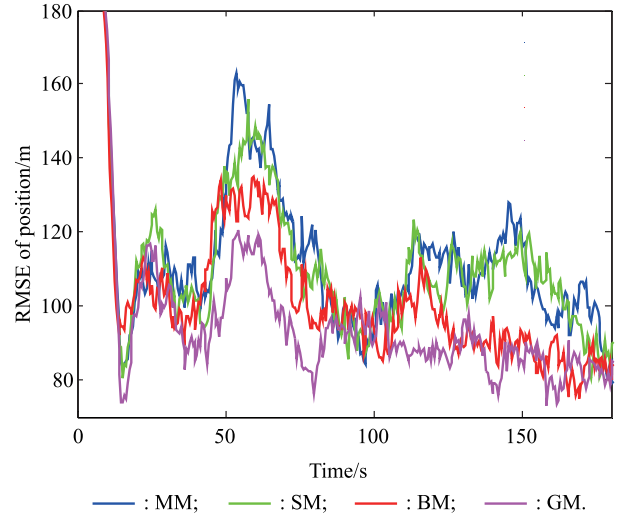


Fig. 2 RMSE of position estimation for different filters

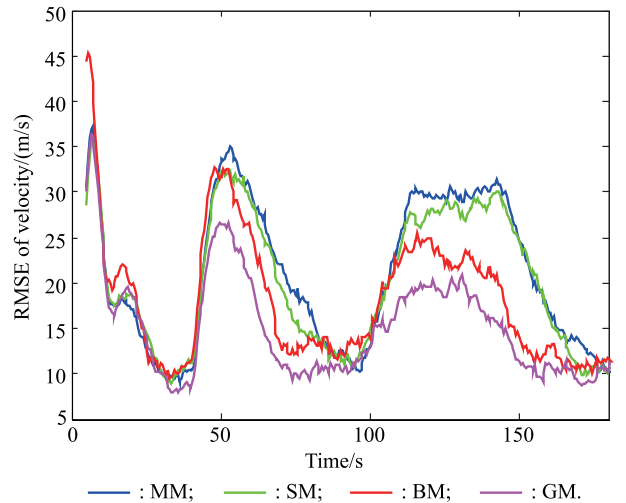


Fig. 3 RMSE of velocity estimation for different filters

Fig. 4 and Fig. 5 show the aerodynamic parameter estimation and the corresponding RMSE results. In order to represent the self-adaption of GM, the guidance commands α_{tg} and α_{cg} (i.e., the expected values of α_t and α_c) are calculated from α_{lg} and φ_g by (11). It can be seen that: (i) When the aerodynamic parameters are changing drastically, the guidance commands decrease or increase rapidly in the direction of the corresponding parameters' change trend; consequently the GM converges faster than

the other three models. The estimation errors of MM and SM are nearly of the same order, the performance of BM is better than those of MM and SM; (ii) When the aerodynamic parameters are changing slightly, the performance differences of the four models are small, and the guidance commands are nearly equal to the estimated aerodynamic parameters.

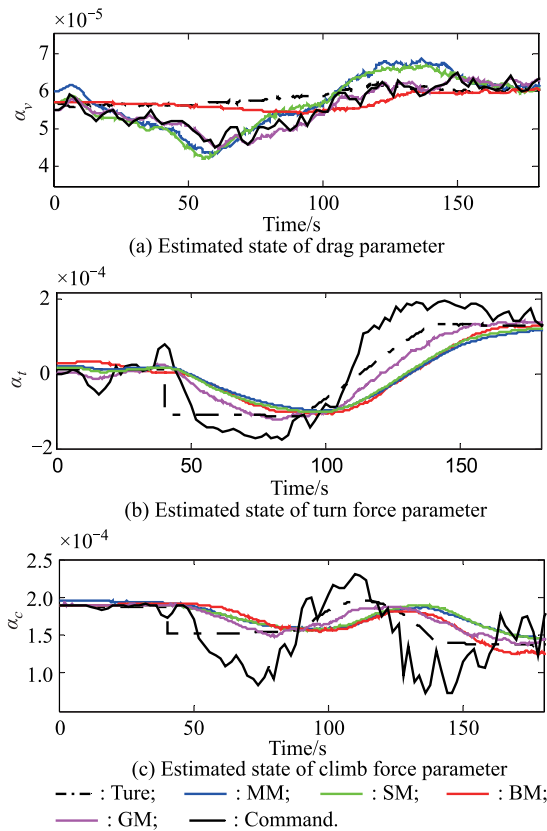


Fig. 4 Aerodynamic parameters estimation of different dynamic models

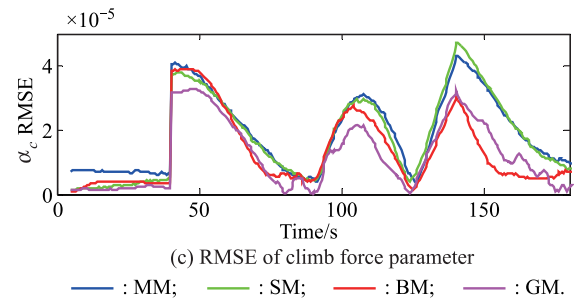
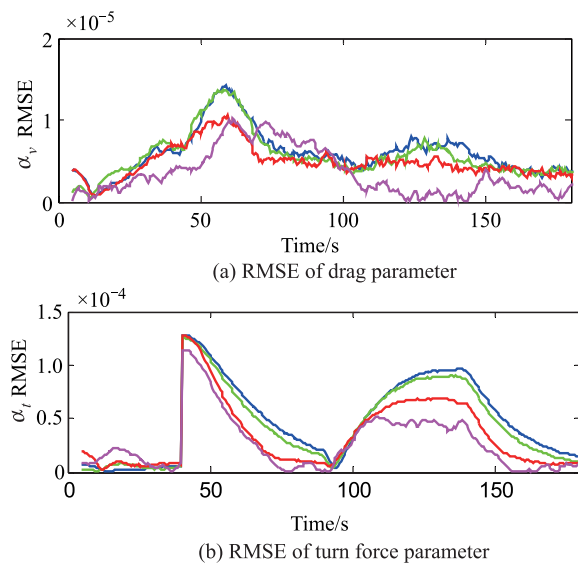


Fig. 5 RMSE in aerodynamic parameter estimation of different dynamic models

Analysis of the above results shows that: (i) The reason why the SM does not show outstanding performance may be that the assumption of harmonic motion is over-constrained for state estimation; (ii) The guidance commands reflect the change trend of maneuver quickly; therefore the GM can adaptively match the flight state online and show better performance.

In order to study the influence of the estimator on these models, a comparative performance assessment with various conditions for different estimators as well as measurement parameters is presented. The cases with various conditions are shown in Table 2.

Table 2 Cases with various conditions for comparison of performance

Case	Estimator	Measurement parameter	
		Noise variance	Sampling period
1	EKF	R	T
2	UKF	R	T
3	EKF	$2R$	T
4	EKF	R	$2T$

Table 3 shows the average RMSEs of estimated states. It can be seen that: (i) Estimation accuracy of UKF is higher than that of EKF, but the performance of the filtering algorithm is not obvious compared with the model; (ii) When the noise variance is doubled, the average RMSEs of position and velocity increase by approximately 100% and 35% respectively, and the average RMSEs of aerodynamic parameters increase by approximately 15%–40%; (iii) When the sampling period is doubled, the average RMSEs of position and velocity increase by approximately 70% and 25%, respectively, and the average RMSEs of aerodynamic parameters increase by approximately 20%–200%.

Analysis of the above simulation shows that: (i) The filter has less influence on the performance of the models, and using EKF as the estimator can improve the computational efficiency; (ii) Reducing the noise variance helps to improve the position and velocity estimation; (iii) Increasing the sampling frequency helps to improve aerodynamic parameter estimation; (iv) Similar to previous results, the SM shows slightly better performance than the MM, and

the BM provides better tracking performance than the SM and the MM. Meanwhile, the GM is the best model among these models, further confirming the conclusion mentioned above.

Table 3 Performance comparison of state estimation errors

Type	Example	Case 1	Case 2	Case 3	Case 4
Position/m	MM	107.8	102.7	192.0	167.6
	SM	105.7	101.5	187.4	160.3
	BM	97.00	92.54	171.3	142.6
	GM	78.11	74.05	151.3	132.6
Velocity/(m/s)	MM	23.94	22.85	37.12	33.59
	SM	23.00	21.47	32.65	32.89
	BM	19.34	18.71	26.80	26.48
	GM	18.64	17.34	26.83	23.48
$\alpha_v/(10^{-6})$	MM	7.069	6.904	9.132	18.04
	SM	6.770	6.548	8.585	17.49
	BM	1.861	1.811	2.047	12.56
	GM	2.861	2.659	4.097	15.82
$\alpha_t/(10^{-6})$	MM	80.85	76.20	86.51	100.7
	SM	77.95	75.25	83.78	97.70
	BM	71.22	69.94	76.37	89.97
	GM	67.76	65.13	70.38	85.87
$\alpha_c/(10^{-6})$	MM	19.86	17.07	21.82	23.25
	SM	20.06	19.05	22.18	23.32
	BM	17.50	17.80	18.35	19.41
	GM	14.20	15.56	16.97	17.50

7. Conclusions

Aiming at handling complicated maneuvers or other unpredicted emergencies, three coupled dynamic models are developed for state estimation of HGV. The novelty of the proposed models lies on some coupled information between guidance variables and aerodynamics: the SM with a harmonic oscillator, the BM with trigonometric functions of bank angle and the GM with changing rule of guidance variables. Compared with the works of the predecessors, the proposed models no longer simply treat the aerodynamic parameters as independent random processes, but model them in consideration with the prior knowledge mentioned above. The new structures can match the aerodynamics better and be closer to the real motion of HGV.

A comparative assessment based on the Monte Carlo method is carried out with different cases. The simulation reveals that the GM produces the best estimation accuracy and the BM shows the second. Notwithstanding consideration of the harmonic motion, the SM does not outperform the MM markedly. This research provides a new idea for how to improve the estimation accuracy of the dynamic model by utilizing the coupled information between guidance variables and aerodynamics.

References

- [1] PAUL L M, VINCENT L R, LUAT T N, et al. NASA hypersonic fight demonstration overview, status, and future plans. *Acta Astronautica*, 2004, 55(7): 619–630.

- [2] DARPA. Tactical boost glide broad agency announcement. DARPA-BAA-14-24, 2014.
- [3] MAHAPATRA P R, MEHROTRA K. Mixed coordinate tracking of generalized maneuvering targets using acceleration and jerk models. *IEEE Trans. on Aerospace and Electronic Systems*, 2000, 36(3): 992–1000.
- [4] LI X R, JILKOV V P. Survey of maneuvering target tracking. Part I: dynamic models. *IEEE Trans. on Aerospace and Electronic Systems*, 2004, 39(4): 1333–1364.
- [5] GHOSH S, BHATTACHARYYA A K, MUKHOPADHYAY S, et al. Improved estimation of kinematic state of reentry ballistic targets with modeling of colored and nonstationary seeker noise. *IEEE Trans. on Aerospace and Electronic Systems*, 2012, 48(4): 3186–3206.
- [6] SUN T, XIN M. Hypersonic entry vehicle state estimation using nonlinearity-based adaptive cubature Kalman filters. *Acta Astronautica*, 2017, 134(3): 221–230.
- [7] WANG G H, LI J J, ZHANG X Y, et al. A tracking model of near space hypersonic slippage leap maneuvering target. *Acta Aeronautica et Astronautica Sinica*, 2015, 36(7): 2400–2410.
- [8] ZHANG X Y, WANG G H, LI J, et al. Tracking of hypersonic sliding target in near-space. *Acta Aeronautica et Astronautica Sinica*, 2015, 36(6): 1983–1994.
- [9] ZHANG X Y, WANG G H, JING Z, et al. Tracking of hypersonic boost-to-glide trajectory target in near-space. *Journal of Astronautics*, 2015, 36(10): 1125–1132. (in Chinese)
- [10] NIE X H, ZHANG F M, XU Y M. Adaptive model algorithm for maneuvering target tracking of NSHV. *Systems Engineering and Electronics*, 2016, 38(3): 506–511. (in Chinese)
- [11] LIANG Y Q, HAN C Z. Hybrid state estimation and model-set design of invariable-structure semi-ballistic reentry vehicle. *Science China: Information Sciences*, 2011, 54(4): 812–823.
- [12] LIANG Y Q, HAN C Z, SUN Y J, et al. Modeling and multiple-model estimation of invariable-structure semi-ballistic reentry vehicle. *Acta Automatica Sinica*, 2011, 37(6): 700–712.
- [13] QIN L, LI J L, ZHOU D. Tracking filter algorithm for near space target based on AGIMM. *Systems Engineering and Electronics*, 2015, 37(5): 1009–1014. (in Chinese)
- [14] QIN L, LI J L, ZHOU D. Tracking for near space target based on IMM algorithm. *Systems Engineering and Electronics*, 2014, 36(7): 1243–1249. (in Chinese)
- [15] LI X R, JILKOV V P. Survey of maneuvering target tracking. Part II: motion models of ballistic and space targets. *IEEE Trans. on Aerospace and Electronic Systems*, 2010, 46(1): 96–119.
- [16] MINVIELLE P. Decades of improvements in re-entry ballistic vehicle tracking. *IEEE Aerospace & Electronic Systems Magazine*, 2005, 20(8): CF/1-CF14.
- [17] FARINA A, RISTIC B, BENVENUTI D. Tracking a ballistic target: comparison of several nonlinear filters. *IEEE Trans. on Aerospace and Electronic Systems*, 2002, 38(3): 854–867.
- [18] OLIVIER D M, ROBERT H B. Tracking and identification of a maneuvering reentry vehicle. *Proc. of the AIAA Guidance, Navigation, and Control Conference and Exhibit*, 2003: 1–11.
- [19] ZHANG S C, HU G D. Target tracking for maneuvering reentry vehicles with interactive multiple model unscented Kalman filter. *Acta Automatica Sinica*, 2007, 33(11): 1120–1125.
- [20] KIM J, VADDI S S, MENON P K, et al. Comparison between nonlinear filtering techniques for spiraling ballistic missile state estimation. *IEEE Trans. on Aerospace and Electronic Systems*, 2012, 48(1): 313–328.
- [21] KIM J, MENON P, OHLMEYER E. Motion models for use with the maneuvering ballistic missile tracking estimators. *Proc. of the AIAA Guidance, Navigation, and Control Conference*, 2010: AIAA 2010–7589.

- [22] ZHANG K, XIONG J J, HAN C Y, et al. A tracking algorithm of hypersonic glide reentry vehicle via aerodynamic model. *Journal of Astronautics*, 2017, 38(2): 123–130. (in Chinese)
- [23] WU N, CHEN L. Adaptive Kalman filtering for trajectory estimation of hypersonic glide reentry vehicles. *Acta Astronautica et Astronautica Sinica*, 2013, 34(8): 1960–1971.
- [24] MOON K R, KIM T H, SONG T L. Comparison of ballistic-coefficient-based estimation algorithms for precise tracking of a re-entry vehicle and its impact point prediction. *Journal of Astronomy & Space Sciences*, 2012, 29(4): 363–374.
- [25] GHOSH S, MUKHOPADHYAY S. Tracking reentry ballistic targets using acceleration and jerk models. *IEEE Trans. on Aerospace and Electronic Systems*, 2011, 47(1): 666–683.
- [26] ZHOU Z, LIU J M, GUO X K. Adaptive tracking algorithm for reentry vehicle based on stochastic model approximation. *Journal of Beijing University of Aeronautics and Astronautics*, 2014, 40(5): 651–657.
- [27] HOUGH M E. Reentry maneuver estimation using nonlinear Markov acceleration models. *Journal of Guidance, Control and Dynamics*, 2017, 40(7): 1–18.
- [28] KARELAHTI J, VIRTANEN K. Adaptive controller for the avoidance of an unknown guided air combat missile. *Proc. of the 46th IEEE Conference on Decision and Control*, 2008: 1306–1313.
- [29] ZOU X G, ZHOU D, DU R L, et al. PN guidance law identification using multi-model adaptive estimation. *Journal of Astronautics*, 2016, 37(8): 619–630. (in Chinese)
- [30] WEISS S S. Identification of nonlinear aerodynamic derivatives using classical and extended local model networks. *Aerospace Science and Technology*, 2010, 42(1): 1–12.
- [31] REGAN F J, ANANDAKRISHNAN S M. *Dynamics of atmospheric re-entry*. New York: AIAA, 1993.
- [32] PHILLIPS T H. *A common aero vehicle (CAV) model, description, employment guide*. Arlington: Schafer Corporation for AFRL and AF-SPC, 2003.

Biographies



hypersonic vehicle tracking.
E-mail: christophzhang@163.com

ZHANG Kai was born in 1990. He received his B.S. degree from School of Aerospace Science and Engineering, National University of Defense Technology in 2014. He is currently working toward his Ph.D. degree in the Air Force Early Warning Academy. So far he has published more than ten papers, in which three papers are indexed by EI. His research interests include information fusion and



XIONG Jiajun was born in 1961. He received his Ph.D. degree from School of Computer, Huazhong University of Science and Technology in 2004. He now is a professor in Air Force Early Warning Academy. So far he has published more than 100 papers, in which more than ten papers are indexed by EI or SCI. His research interests are early-warning intelligence analysis, and information fusion.
E-mail: jiajunxiong@yahoo.com



FU Tingting was born in 1988. She received her B.S. degree from School of Optoelectronic Science and Engineering, National University of Defense Technology in 2014. She now is a lecturer in Air Force Early Warning Academy. Her research interests include information fusion and systems engineering.
E-mail: 124611796@qq.com